AEOLIAN LANDFORMS IN THE EXOMARS 2028 LANDING SITE. S. Silvestro[1,2], D.A. Vaz[3,1], F.M. Grasso[4], U. Rizza[4], L.K. Fenton[2], R. Cardoso[3], A. Pacifici[5], D. Tirsch[6], E. A. Favaro[7], Y. Tao[8], F. Salese[5], C.I. Popa[1], G. Franzese[1], G. Mongelluzzo[1], C. Porto[1], M. Pajola[9], F. Esposito[1]. [1]INAF, Osservatorio Astronomico di Capodimonte, Napoli, Italy (simone.silvestro@inaf.it). [2]SETI Institute, Mountain View, CA, USA. [3]CITEUC, University of Coimbra, Portugal. [4]CNR ISAC Lecce, Italy. [5]IRSPS, Univ. G. d'Annunzio, Chieti-Pescara, Italy, [6]Inst. Planetary Res., DLR, Berlin, Germany. [7]ESA/ESTEC, Noordwijk, the Netherlands. [8]Freie Univ., Berlin, Germany. [9]INAF, Osservatorio Astronomico di Padova, Italy.

Intro & Methods: ESA's ExoMars Rosalind Franklin Mission will land a rover at Oxia Planum to search for signs of life on Mars [1, 2]. Bright bedforms (Transverse Aeolian Ridges [TARs]), and erosive wind-formed ridges (Periodic Bedrock Ridges [PBRs]) have been documented in the landing site [3-6]. In this study, we compare automated and manual mapping of aeolian features in CTX (6 m/pixel), CaSSIS (5 m/pixel) and HiRISE (25 cm/pixel) images in the landing site (Fig. 1) with sand fluxes from the NASA Ames GCM [7] obtained with the Martian Surface/Atmosphere Web Interface [8]. In particular, we focus our attention on bright bedforms, ridges and wind streaks (Fig. 1). Since these features are widespread on Mars, the observations made here on ridge and bedform are also relevant to other areas and landing sites [9-13].

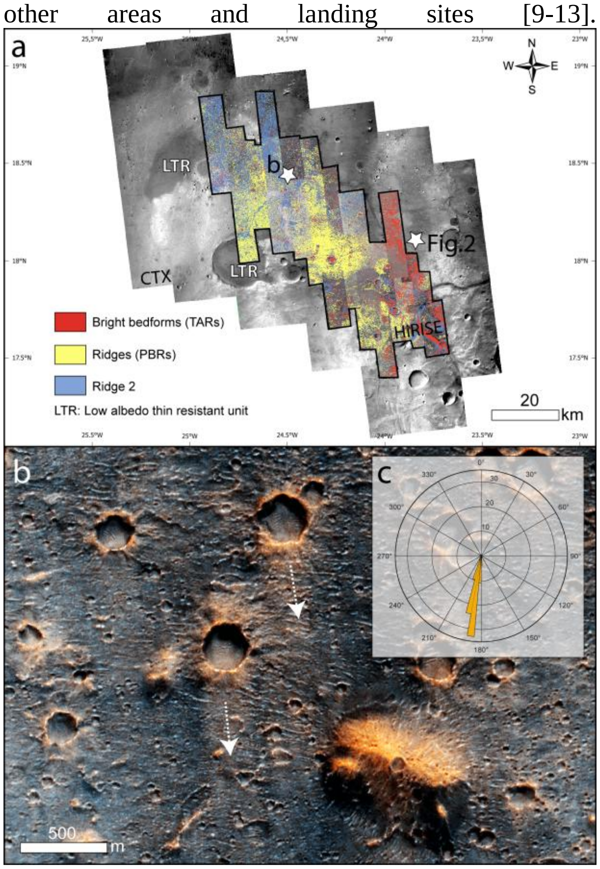

Fig. 1: (a) Automatically mapped ridges and TARs within the study area (CTX and HiRISE mosaics [15]). **(b, c)** Wind streak orientations in the landing area (CaSSIS RGB image MY35_007623_019_0).

Results: Different aeolian features are observed in the landing area, including a new class of ridges (*Ridge 2*) identified thanks to the new automatic mapping methodology employed in this work (Fig. 1a). *Wind streaks* (n = 87) were manually mapped on the CTX image mosaic [15] in a GIS environment. Most of the mapped streaks are bright-toned (n = 85), indicating winds originating from the NNW–NNE (Fig. 1b, c). A few dark-toned streaks (n = 2), formed by winds from the E–ESE, were also identified. *Bright bedforms* (TARs) were automatically mapped within the study area using the method described in [16]. They are widespread, especially in the SE, suggesting a higher sand supply and availability. *Ridges* (PBRs) were automatically mapped as well (Fig. 1a). These features are bright-toned as they are directly carved into the clay-enriched Noachain bedrock [4-6]. *Ridge 2:* Together with the bright-toned ridge set, here we identified a new class of WNW–ESE-oriented cratered ridges (Figs 1 & 2). These features are mostly located in the NW of the study area but can also be found elsewhere (Fig. 2). Theses sets of ridges display Y-junctions, can be found inside degraded impact craters, and may be locally covered by boulders from nearby impacts [4]. However, unlike PBRs, they are not directly carved into the underlying bedrock (Fig. 2). Interestingly, these ridge sets are also observed within craters on the low albedo thin resistant (LTR) unit [4], which is widespread in Oxia Planum [15, 17] (Fig. 1).

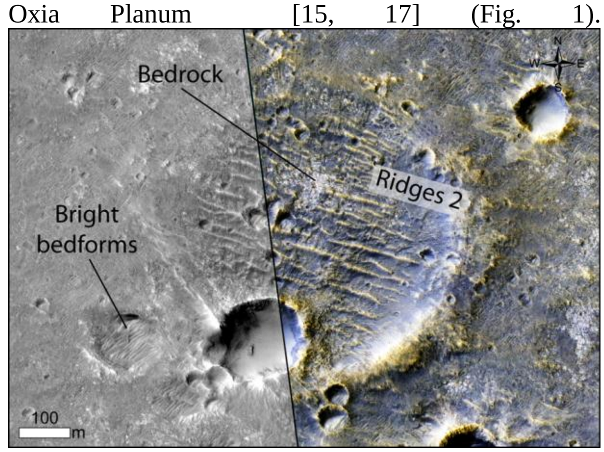

Fig. 2: WNW-ESE ridges (Ridge 2) inside an eroded impact crater (HiRISE ESP_062481_1985). The ridges directly overlay the bright, clay-bearing Noachian bedrock [2].

Discussion: The consistent orientation of bright wind streaks in the study area suggests contemporary regional winds predominantly blowing from the north, corresponding to the return flows of the Hadley cell circulation [18]. We also identified a secondary mode formed by winds from the ESE. Interestingly, a bimodal sand flux direction is also predicted by the GCM (Fig. 3), with one mode (~172°–188°) closely matching the observed bright-toned wind streak orientations (Fig. 1b, c). This, along with no observed changes in orientation or modification of the bright streaks, indicates that these winds continue to blow at the surface and/or that winds from other directions are not strong or frequent enough to rework the wind streaks.

Bright bedforms (TARs) are likely relict or static features shaped by past wind conditions [4, 5]. This is supported by the GCM-predicted bedform orientation (red line in Fig. 3), which does not align with either the observed TARs' orientation or that of the older periodic bedrock ridges (PBRs) [4-6].

The newly identified "Ridge 2" class of landform has previously been interpreted as precursor bedforms that initiated the formation of the underlying PBRs [4]. This interpretation is supported by (1) the close spatial association between PBRs and the "ridge 2" class, and (2) their similar orientation. However, in the example shown in Fig. 2, the ridges are located on a flat bedrock surface and are not associated with PBRs. This observation raises the possibility that these features may represent a later episode of aeolian deposition or erosion, occurring after the formation of the PBRs [4]. This hypothesis is consistent with the new automatic mapping performed here, with the presence of the "ridge 2" class inside craters over the LTR unit (indicating post-dating of the unit emplacement) and recent age estimates for the PBRs [6]. The morphology of the "Ridge 2" class varies across the study area, with some ridges appearing subdued and eroded making them similar to ghost-dune pits [19]. Alternatively, such a relationship between positive and subdued morphologies might represent an assemblage of erosional scars and bedforms, similar to those observed at Meridiani Planum (see Fig. 6b in [10]). In this scenario, ridges are thought to have migrated southwest, leaving behind erosional scars.

Detailed examination of the relationships among ridges and TARs by the RFM rover will be crucial for advancing our understanding of ridges and PBR formation mechanisms [20, 21], the winds responsible for shaping TARs, and broader Martian climatic changes [9, 10].

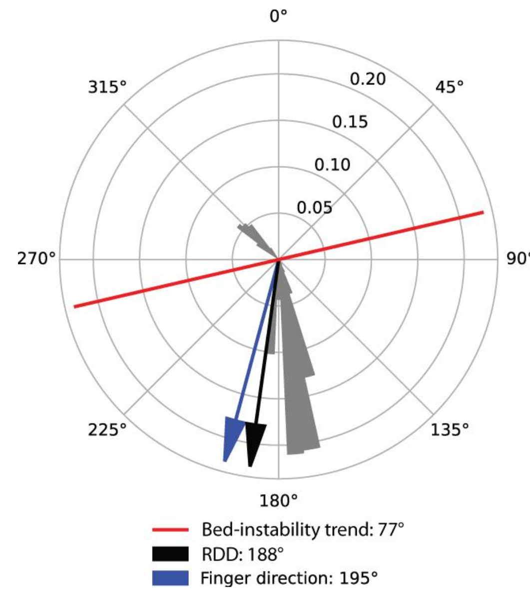

Fig. 3: GCM output at 18.2°N, 24.3°W. RDD represents the resultant drift direction [22]. The red line indicates the predicted orientation assuming the bed-instability mode as the bedform formation model [23, 24]. "Finger direction" refers to the bedform elongation direction, assuming the fingering mode as the formation mechanism [24].

References: [1] Vago J. et al. (2017). *Astrobiology, 17*. [2] Quantin et al. (2021), *Astrobiology, 21*. [3] Balme M. et al. (2017), *PSS, 153*, 39-53. [4] Silvestro S. et al. (2021), *GRL, 48*. [5] Favaro E. et al. (2021), *JGR, 126*. [6] Favaro E. et al. (2024), *EPSL, 626*. [7] Haberle R.M. et al. (2003), *Icarus, 161*. [8] Grasso F.M. et al. (2025), *this issue*. [9] Golombek M. et al. (2010), *JGR, 115*, 1-34. [10] Fenton L.K. et al. (2018), *JGR, 123*, 1–15. [11] Stack K.M. et al. (2022), *JGR, 127*, e2021JE007096. [12] Sullivan et al. (2022), *53rd LPSC*, 2887. [13] Lu Y. et al. 2022, *EPSL, 595*, 117785. [14] Gou S. et al. 2022, *EPSL, 595*, 117764. [15] Fawdon et al. (2024), *Journal of Maps, 20(1)*, 2302361. [16] Vaz D.A. et al. (2023), *EPSL, 614*. [17] Harris E. et al. (2024), *JGR, 129*. [18] Greeley et al. (1993), *JGR, 98*, E2, 3183-3196. [19] Day M.D. & Catling D.C. (2018), *JGR, 123*. [20] Montgomery D.R. et al. (2012), *JGR, 117*, E03005. [21] Hugenholtz C.H. et al. (2015), *Aeol. Res., 18*, 135–144. [22] Fryberger S.G. & Dean G. (1979), *USGS prof. paper, 1052*. [23] Rubin D.M. & Hunter R.E. (1987), *Science, 237*. [24] du Pont S.C. et al. (2014), *Geology, 42*. **Acknowledgement:** The results reported here were obtained in the context of the Earth-Moon-Mars (EMM) project, led by INAF in partnership with ASI & CNR, funded under the National Recovery and Resilience Plan, Mission 4, Component 2, Investment 3.1: "Fund for the realisation of an integrated system of research and innovation infrastructures" Action 3.1.1 funded by the EU, NextGenerationEU.